

TrustGeoGen: Scalable and Formal-Verified Data Engine for Trustworthy Multi-modal Geometric Problem Solving

Daocheng Fu^{1,2*} Zijun Chen^{2,3*} Renqiu Xia^{2,3*} Qi Liu^{2,3} Yuan Feng^{2,3} Hongbin Zhou²
Renrui Zhang² Shiyang Feng² Peng Gao² Junchi Yan³ Botian Shi² Bo Zhang^{2†} Yu Qiao²

¹Fudan University, ²Shanghai Artificial Intelligence Laboratory, ³Shanghai Jiao Tong University
{fudaocheng, zhangbo}@pjlab.org.cn, {chenzijun, xiarenqiu}@sjtu.edu.cn

Abstract

Mathematical geometric problem solving (GPS) often requires effective integration of multimodal information and verifiable logical coherence. Despite the fast development of large language models in general problem solving, it remains unresolved regarding with both methodology and benchmarks, especially given the fact that existing synthetic GPS benchmarks are often not self-verified and contain noise and self-contradicted information due to the illusion of LLMs. In this paper, we propose a scalable data engine called TrustGeoGen for problem generation, with formal verification to provide a principled benchmark, which we believe lays the foundation for the further development of methods for GPS. The engine synthesizes geometric data through four key innovations: 1) multimodal-aligned generation of diagrams, textual descriptions, and stepwise solutions; 2) formal verification ensuring rule-compliant reasoning paths; 3) a bootstrapping mechanism enabling complexity escalation via recursive state generation and 4) our devised GeoExplore series algorithms simultaneously produce multi-solution variants and self-reflective backtracking traces. By formal logical verification, TrustGeoGen produces GeoTrust-200K dataset with guaranteed modality integrity, along with GeoTrust-test testset. Experiments reveal the state-of-the-art models achieve only 49.17% accuracy on GeoTrust-test, demonstrating its evaluation stringency. Crucially, models trained on GeoTrust achieve OOD generalization on GeoQA, significantly reducing logical inconsistencies relative to pseudo-label annotated by OpenAI-o1. Our code is available at <https://github.com/Alpha-Innovator/TrustGeoGen>.

1. Introduction

Geometric Problem Solving (GPS), as a pivotal branch of mathematical reasoning or more broadly speaking, general reasoning, demands tripartite capabilities [40]: 1) extracting spatial relationships from visual diagrams, 2) performing mathematical reasoning in language modality, and 3) maintaining stepwise logical coherence where intermediate conclusions rigorously justify subsequent deductions. The development of trustworthy AGI systems fundamentally relies on reliably annotated multimodal data that not only bridges visual-textual modalities but also preserves closed-loop reasoning chains. This requirement stems from a critical axiom: a geometrically valid solution demands both correct answers and air-tight logical pathways, as human experts reject proofs with *leap-of-faith** arguments even when final results are accurate.

The recent advancement of Multimodal Large Language Models (MLLMs) [4, 8, 11, 12, 14, 20, 22, 24, 27, 28, 30, 37, 40, 45] has revealed promising capabilities in geometric reasoning, demonstrating competence in solving elementary geometric problems. Parallel developments in external formalized expert systems [7, 18, 21, 44] have extended problem solving capabilities to more complex geometric configurations, with highly specialized models [9, 35, 43] even approaching challenges of the International Mathematical Olympiad (IMO) level. However, these achievements are critically dependent on high-quality geometric data, currently in short supply. The existing datasets are mainly derived from manual annotations of secondary school textbook problems [6, 7, 15, 21, 44], and this process is limited in scale and diversity. Although recent integration of MLLMs (e.g. GPT series [2, 23, 24]) for synthetic question-answer generation [14, 46] has partially ameliorated data scarcity concerns, significant challenges persist in ensuring

*Equal contribution

†Corresponding author.

*Here it means an unjustified or unsubstantiated jump in reasoning, where a conclusion is reached with insufficient logical steps or evidence.

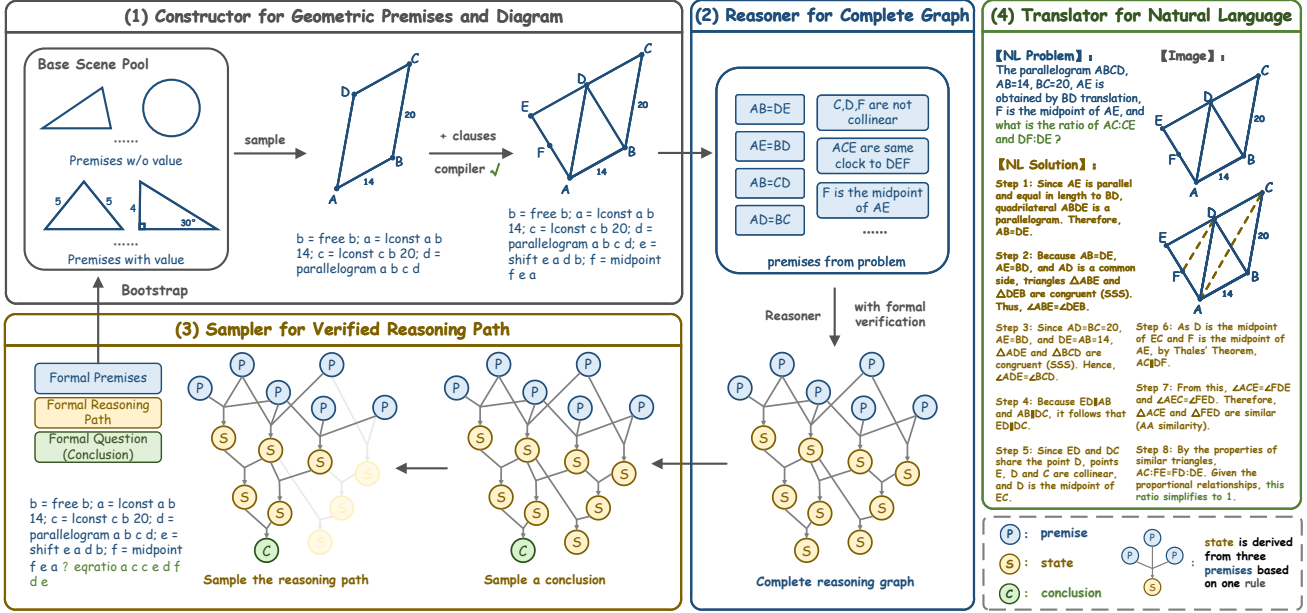


Figure 1. TrustGeoGen overview: (1) **Constructor** builds geometric premises from a base scene by incrementally adding clauses and enforces constraints via a compiler, (2) **Reasoner** generates rigorously validated reasoning graph from premises by geometric rules, (3) **Sampler** selects conclusion nodes from the graph and traces reasoning paths to formalize problems and solutions, (4) **Translator** converts formal language to natural language for metadata. A bootstrap mechanism further enhances data complexity and problem difficulty.

stepwise solution validity[†], which may undermine the logical coherence of reasoning chains during model training.

However, current geometric datasets exhibit four deficiencies: 1) **Modality Fragmentation**: existing datasets suffer from incomplete modality alignment, lacking comprehensive annotations that synchronize images, textual captions, questions, and chain-of-thought reasoning processes within unified instances. 2) **Scalability Issues**: Most approaches rely on repurposing human-authored problems from textbooks or examinations rather than generating novel, curriculum-aligned challenges. 3) **Cost Constraints**: Manual annotation requires costly geometry expertise, while generating solutions through MLLMs consumes excessive computational resources. 4) **Trust Deficits**: Model-generated solutions lack reliable automated verification mechanisms, introducing risks of undetected logical errors or misaligned reasoning steps.

To this end, we develop **TrustGeoGen**, a formal language-verified geometric data generation engine that autonomously produces geometric problems, diagrams, and stepwise solutions through four integrated components: 1) a *Constructor* to generate constraint-satisfying problem premises and diagrams, 2) a *Reasoner* expanding geometrically valid reasoning graphs with rigorous node verification, 3) a *Sampler* leveraging the algorithm *GeoExplore* to ex-

[†]Specifically, automatically generated procedural labels frequently contain latent inconsistencies, such as misapplied geometric axioms or diagram-coordinate mismatches.

tract high-quality reasoning paths, which are later converted into problems by pairing initial premises with derived conclusions, and 4) a *Translator* rendering formal specifications into natural language. Furthermore, we improve the problem complexity through a bootstrapping mechanism in TrustGeoGen, where formally verified geometric premises in prior stages are recursively fed back to the *Constructor* to iteratively append new premises. This closed-loop process enables systematic escalation of difficulties while maintaining logical consistency. Additionally, we refine the algorithm *GeoExplore* to simultaneously explore alternative solution paths and self-correcting reasoning trajectories, generating problems with multiple valid solutions and self-reflective traceback data.

Our proposed TrustGeoGen ensures: 1) **Modality Completeness** with synchronized dual-form (formal & informal) captions, questions, solutions, and diagrams, 2) **Scalability** in generating geometry problems by bootstrapping mechanisms without reliance on existing data source and 3) **Verifiability** through formal validation of all solution steps in its integrated reasoner. Based on TrustGeoGen, we develop a dataset *GeoTrust* containing 200K samples and a compact testset *GeoTrust-test* with 240 samples. Experimental results demonstrate state-of-the-art reasoning models DeepSeek-R1 [10] and OpenAI-o1 [25] achieve only 45.00% and 49.17% accuracy respectively on *GeoTrust-test*. Furthermore, training with our strictly verified reasoning step annotation data proves to be more effective com-

pared to using *pseudo-labels*[‡] with unverifiable reasoning processes. Additionally, our training data from GeoTrust enhances model performance on the out-of-distribution (OOD) testset GeoQA [6], highlighting its broader generalization capability. In a nutshell, our contributions are as follows.

- We develop **TrustGeoGen**, a formalized geometric data generation engine, producing scalable and multimodal-integrated data (geometric diagrams, formal & natural language captions, questions and solutions) with trustworthy reasoning guarantees via formal verification.
- By introducing a bootstrap mechanism, we iteratively generate data with more complex premises and longer reasoning chains, enabling automated complexity scaling.
- Our *GeoExplore* series algorithms generates multi-solution problems and self-reflective traceback data, enriching diversity while ensuring trustworthiness.
- We construct the dataset *GeoTrust* with 200K samples and *GenTrust-test* testset, dynamically generated without dependency on prior data sources, ensuring unbiased and extensible evaluating capabilities.
- Experiments demonstrate that existing MLLMs significantly underperform on high-difficulty geometric reasoning tasks, and our verified data exhibit effectiveness and generalization as training source.

2. Methodology

The data engine TrustGeoGen serves as the core for constructing high-quality geometric reasoning datasets, enabling the generation of complex geometric scenes and reasoning paths to support robust and scalable inference.

2.1. Data Engine

In the process of generating multi-modal geometric reasoning data, it employs a rule-based data construction method augmented by a geometric verifier to synthesize high-quality and scalable datasets. This approach ensures that the data is accurate, controllable, and scalable. As shown in Fig. 1, our framework consists of four components: Constructor, Reasoner, Sampler, and Translator.

Constructor starts the data construction process by building geometric scenes. It incrementally adds new conditions to a basic geometric scene, thus constructing increasingly complex scenes. In TrustGeoGen, a basic geometric scene consists of simple geometric shapes (e.g., triangles, circles, parallelograms) and their associated numerical information (e.g., side lengths, radii, angles). When a base scene is created, it contains an initial set of geometric premises $P_{base} = \{p_i^g, p_j^d\}$, where p_i^g represents geometric relationship conditions (e.g., $AB \parallel CD$) and p_j^d repre-

sents numerical conditions (e.g., $\angle BAC = 30^\circ$). Subsequently, the Constructor incrementally adds new premises to the base scene, increasing its complexity while expanding the premise set P . Notably, the Constructor requires that each newly added premise must be connected to the preceding scene to ensure the overall geometric scene remains cohesive and connected. By controlling the number of new premises added, the Constructor generates geometric scenes of varying complexity levels. Each constructed scene is then validated by a geometric compiler [31] to ensure the validity of its geometric relationships. Finally, the process yields a geometric scene with a specified level of complexity and an expanded premise set $P = \{p_{i+m}^g, p_{j+n}^d\}$.

Reasoner leverages a predefined set of geometric theorems to infer new states from premises generated by the *constructor*, formulating a reasoning graph:

$$\mathcal{G} = (S, S_0, R, \hookrightarrow) \quad (1)$$

- S is the set of states, where each state $s \in S$ represents a derived conclusion or fact in the reasoning process.
- $S_0 = P \subseteq S$ is the set of initial states (the premises P generated by the *constructor*).
- R is the set of rules, where each rule $r \in R$ defines a logical inference relationship between states.
- $\hookrightarrow \subseteq S \times R \times S = \{(S_r, r, s') \mid S_r \subset S, r \in R, s' \in S\}$ is the state transition relation. A transition $S_r \xrightarrow{r} s'$ indicates state s' is derived from s by applying rule r .

Reasoning begins with the initial states $S_0 = P$ (given premises from the **constructor**), forming the root nodes of the graph \mathcal{G} . The graph expands by applying inference rules to existing states. For every state set $S_r \subset S$ and rule $r \in R$, if r can be applied to S_r to derive a new state s' (formally $S_r \xrightarrow{r} s'$), the reasoner performs two atomic updates: 1) Add the new state S_r to S and 2) Add the edges (S_r, s') to the transition relation \hookrightarrow with rule r . Finally, the complete graph is the smallest closure satisfying:

$$S = S_0 \cup \left\{ s' \mid \forall S_r \subset S, r \in R, S_r \xrightarrow{r} s' \right\} \quad (2)$$

Sampler operates on the reasoning graph \mathcal{G} by sampling a target state s_n and subsequently searching for its path:

$$\mathcal{P} = \{(S_{i-1}, r_s, s) \mid \forall s \in S_i, S_{i-1} \xrightarrow{r_s} s, i = n, \dots, 1\} \quad (3)$$

where each triplet (S_i, r_s, s) denotes a specific transition during the reasoning process, derived by applying rule r_s to state set S_{i-1} to produce state s . Any state s_n within the state set S can be treated as a problem to solve in order to derive a reasoning path \mathcal{P} . The sampler is initialized with a state $s \in S_n$ to retrieve the corresponding transition rule r_s and the upstream dependent states S_i . This process is repeated iteratively until the state set S_i consists entirely of initial premises S_0 . At that point, the full reasoning path has been successfully constructed. Notably, during the graph

[‡]Here, pseudo-label means that the solution to a given question is annotated using SOTA MLLMs (e.g. OpenAI-o1 [25]).

Algorithm 1 GeoExplore

Input: Reasoning graph $\mathcal{G} = (S, S_0, R, \leftrightarrow)$, target state s_n , threshold τ_l , threshold τ_r
Output: Filtered reasoning path \mathcal{P}

- 1: **Initialize** $\mathcal{P} \leftarrow \emptyset$
- 2: $s \leftarrow s_n$
- 3: **while** $s \notin S_0$ **do**
- 4: Identify rule $r_s \in R$ and parent state set $S_{i-1} \subset S$ such that $S_{i-1} \xrightarrow{r_s} s$
- 5: Append transition (S_{i-1}, r_s, s) to \mathcal{P}
- 6: $s \leftarrow S_{i-1}$
- 7: **end while**
- 8: Assess path length: $L \leftarrow |\mathcal{P}|$
- 9: Compute premises ratio: $R_P \leftarrow |S_P|/|S_0|$, where $S_P \subseteq \mathcal{P}$
- 10: **if** $L \geq \tau_l$ **and** $R_P \geq \tau_r$ **then**
- 11: **Return** \mathcal{P}
- 12: **else**
- 13: **Discard** \mathcal{P}
- 14: **end if**

construction process in the **Reasoner**, once a state s is derived through rule r_s , no additional state transition relations are appended to s . Consequently, the **Sampler** is always able to identify a unique inference rule r_s corresponding to any state s , thereby guaranteeing the absence of cycles in the reasoning path.

To ensure the quality of the reasoning paths, the **Sampler** employs two metrics to filter out unsuitable paths. The first metric evaluates the length of the reasoning path \mathcal{P} against a predefined threshold τ_l . If the length of \mathcal{P} exceeds τ_l , the path is considered difficult enough. Formally, this condition is expressed as $|\mathcal{P}| \geq \tau_l$, where $|\mathcal{P}|$ denotes the number of transitions in the reasoning path \mathcal{P} . The second metric assesses the ratio of the states in the reasoning path \mathcal{P} that are derived from the initial premises set S_0 . If this ratio exceeds a predefined threshold τ_r , the path is deemed sufficient enough. This condition is formally defined as $\frac{|S_P|}{|S_0|} \geq \tau_r$, where $|S_P|$ represents the number of initial premises used in the reasoning path \mathcal{P} , and $|S_0|$ is the number of all initial premises. By applying these two metrics, the **Sampler** ensures that only high-quality reasoning paths are retained, thereby maintaining the integrity and usefulness of the generated data. The detailed procedure of the aforementioned reasoning path exploration and filtering algorithm, *GeoExplore*, is presented in Algorithm 1.

Translator is responsible for converting the reasoning path \mathcal{P} into a human-readable natural language explanation. To accomplish this, the Translator leverages a large language model (LLM) to "smooth" the reasoning path. For each state and rule in the reasoning path \mathcal{P} , the Translator provides the LLM with a detailed natural language inter-

Algorithm 2 GeoExplore-M

Input: Reasoning graph $\mathcal{G} = (S, S_0, R, \leftrightarrow)$, target state s_n , threshold τ_l , threshold τ_r , number of searches n
Output: Set of filtered reasoning paths \mathcal{P}_{set}

- 1: **Initialize** $\mathcal{P}_{\text{set}} \leftarrow \emptyset$
- 2: **Initialize** used_options $\leftarrow \emptyset$
- 3: **while** True **do**
- 4: **Initialize** $\mathcal{P} \leftarrow \emptyset$
- 5: $s \leftarrow s_n$
- 6: **while** $s \notin S_0$ **do**
- 7: Identify set of rules $\mathcal{R}_s \subseteq R$ and corresponding parent state sets $\mathcal{S}_{i-1}^m \subseteq S$ such that $\forall r_s \in \mathcal{R}_s, \exists S_{i-1} \in \mathcal{S}_{i-1}^m : S_{i-1} \xrightarrow{r_s} s$
- 8: Select $r_s \in \mathcal{R}_s$ and $S_{i-1} \in \mathcal{S}_{i-1}^m$ (choose different options in different searches)
- 9: used_options \leftarrow used_options $\cup \{(r_s, S_{i-1})\}$
- 10: **if** $(S_{i-1}, r_s, s) \notin \mathcal{P}$ **then**
- 11: $\mathcal{P} \leftarrow \mathcal{P} \cup (S_{i-1}, r_s, s)$
- 12: **end if**
- 13: $s \leftarrow S_{i-1}$
- 14: **end while**
- 15: Assess path length: $L \leftarrow |\mathcal{P}|$
- 16: Compute premises ratio: $R_P \leftarrow |S_P|/|S_0|$, where $S_P \subseteq \mathcal{P}$
- 17: **if** $L \geq \tau_l$ **and** $R_P \geq \tau_r$ **then**
- 18: $\mathcal{P}_{\text{set}} \leftarrow \mathcal{P}_{\text{set}} \cup \{\mathcal{P}\}$
- 19: **end if**
- 20: **if** used_options contains all possible options **then**
- 21: **Break**
- 22: **end if**
- 23: **end while**
- 24: **return** \mathcal{P}_{set}

pretation of the geometric states and inference rules, ensuring that the LLM fully understands the semantic and logical meaning of the components in \mathcal{P} . Additionally, the Translator utilizes a few-shot learning strategy to enhance translation accuracy and consistency. Specifically, it includes a pre-curated set of high-quality human-generated translations as few-shot examples, which serve to guide the LLM in generating precise and context-appropriate explanations. By iteratively processing each triplet $(S_{i-1}, r_s, s) \in \mathcal{P}$, the Translator generates a coherent chain-of-thought explanation that mirrors the logical flow of the reasoning graph \mathcal{G} . This ensures that the resulting translation not only reflects the exact logical derivations but also facilitates human understanding by articulating complex geometric relationships in an accessible and comprehensive manner.

2.2. Bootstrap Augmentation

As previously described, TrustGeoGen begins by constructing a complex geometric figure from a completely random

initial scenario and then derives reasoning paths for this instance. While this approach is scalable, its efficiency in generating high-quality data is relatively low, as it may randomly produce geometric scenarios that fail to yield meaningful or valuable results. To address this, TrustGeoGen employs an iterative bootstrap strategy to guide the generation process, thereby improving the efficiency of producing high-quality data. In each iteration, TrustGeoGen utilizes the metrics from the Sampler to evaluate the quality of sampled data on a given graph G . If the average quality of the sampled data on a particular graph G is sufficiently high, TrustGeoGen selects this data as the basis for the subsequent iteration’s initial scenario. Specifically, the process can be represented as $P'_{base} = P = \{p_{i+m}^g, p_{j+n}^d\}$, where P serves as the starting point. The Constructor then incrementally adds new premises to this foundation, increasing the complexity of the scenario. This leads to the generation of $P' = \{p_{i+m+x}^g, p_{j+n+y}^d\}$. Following this, the Reasoner, Sampler, and Translator collaboratively work to complete graph construction, problem-solving, and translation, ultimately producing a new batch of high-quality data.

2.3. Multi-solution Data

In the field of GPS, exploring multiple solutions to a given problem is a crucial method for understanding geometric relationships in depth. By investigating different solution logics, a model can examine geometric scenarios from various perspectives, achieving a comprehensive understanding of the relationships among geometric elements. TrustGeoGen facilitates the construction of multi-solution datasets for specific geometric scenarios through the graph-building procedure of the modify Reasoner and the solving procedure of the Sampler.

During the graph construction phase, in order to obtain multiple solutions, for each state s , when the Reasoner repeatedly identifies transitions in the form $S_r \xrightarrow{r} s$, each identified transition is retained. This retention of multiple transitions provides potential paths for exploring diverse solutions. In the solving process, the Sampler employs an adaptive search algorithm to generate reasoning paths. For any given problem s_n , the Sampler performs multiple path searches. If a state s_i has multiple outgoing transitions, the Sampler selects a different transition at each iteration for the next reasoning step. Consequently, the reasoning paths obtained during these iterations will differ. It is worth noting that to ensure the generated reasoning paths are acyclic, the Sampler enforces a constraint during path construction. Specifically, when attempting to add a triplet (S_i, r_s, s) to the reasoning path \mathcal{P} , the Sampler checks whether this triplet already exists in \mathcal{P} . If it does, the state s is not revisited, thereby preventing cyclical paths in the reasoning process. For details of the multi-solution path searching algorithm, *GeoExplore-M*, refer to Algorithm 2.

Algorithm 3 GeoExplore-T

Input: Directed graph $\mathcal{G} = (S, S_0, R, \leftrightarrow)$, target state $s_t \in S$, threshold τ_p

Output: Trace-back reasoning data \mathcal{D}

- 1: Initialize $\mathcal{D} \leftarrow \emptyset$
 - 2: Compute all reasoning paths $\mathcal{P}_{set}^t = \{\mathcal{P}_1^t, \mathcal{P}_2^t, \dots\}$ to s_t using Algorithm 2
 - 3: Randomly sample a state $s_e \in S$ such that $s_e \notin \text{UpstreamDependencies}(\mathcal{P}^t)$ for any $\mathcal{P}^t \in \mathcal{P}_{set}^t$
 - 4: Search for a reasoning path \mathcal{P}^e leading to s_e
 - 5: **if** $\exists \mathcal{P}^t \in \mathcal{P}_{set}^t, \text{Overlap}(\mathcal{P}^e, \mathcal{P}^t) \geq \tau_p$ **then**
 - 6: Add $\mathcal{P}^e \cup \mathcal{P}^t$ to \mathcal{D}
 - 7: **end if**
 - 8: **return** \mathcal{D}
-

2.4. Self-reflective Traceback Data

Recent studies on the reasoning capabilities of large models suggest that these models acquire substantial knowledge during the pre-training phase. By providing training data with various cognitive templates during the post-training phase, the models can better utilize their inherent knowledge, thereby enhancing reasoning ability and improving response quality[41, 42]. Among these cognitive templates, self-reflection trace-back reasoning serve as highly effective approaches. However, self-reflection and retrospective reasoning often occur during the author’s cognitive process and are rarely preserved in the final outputs, making the collection of relevant data particularly challenging. These types of data are even more scarce in the domain of multi-modal geometric problem-solving.

TrustGeoGen defines trace-back reasoning data as a sub-graph of $\mathcal{G} = (S, S_0, R, \leftrightarrow)$, characterized as the union of sub-graphs with identical upstream dependencies but differing final states. Specifically, for a given piece of trace-back reasoning data, the process involves first deriving an incorrect final state, then retrospectively navigating a correct reasoning path (shared by both the incorrect and correct paths), and ultimately arriving at the correct final state. To achieve this, TrustGeoGen selects a target state s_t and employs Algorithm 2 to enumerate all possible reasoning paths $\mathcal{P}^t \in \mathcal{P}_{set}^t$. Next, a state s_e is randomly sampled from the state set S , ensuring that s_e does not belong to the upstream dependencies of any \mathcal{P}^t . Subsequently, TrustGeoGen searches for a reasoning path \mathcal{P}^e leading to s_e . If \mathcal{P}^e overlaps with any $\mathcal{P}^t \in \mathcal{P}_{set}^t$ and the overlapping portions exceed the threshold τ_p , TrustGeoGen outputs $\mathcal{P}^e \cup \mathcal{P}^t$ as trace-back reasoning data. Notably, Algorithm 2 is utilized to identify all possible reasoning paths for s_t to ensure that s_e does not appear in any potential upstream dependencies, thereby maintaining the integrity of the reasoning process leading to s_t . The details of the trace-back data acquisition algorithm, *GeoExplore-T*, are presented in Algorithm 3.

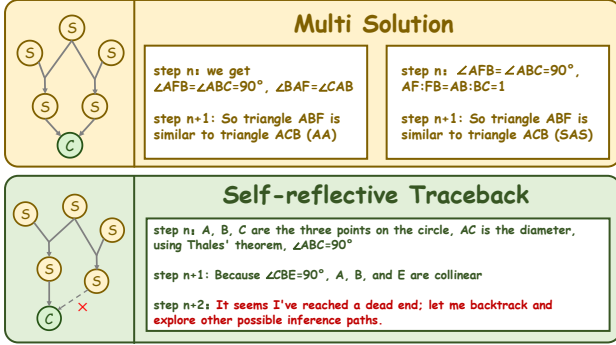


Figure 2. Simple examples of Multi-solution and Self-reflective traceback data.

3. Data Analysis

The modality-completed trustworthy geometric reasoning data holds great potential for improving the geometric problem-solving capabilities of MLLMs. Moreover, it could generalize these abilities to other tasks requiring deep reasoning. To validate it, we utilized TrustGeoGen to produce the dataset *GeoTrust* of 200K samples, from which 8K were sampled as the training set. Additionally, we employed different thresholds, τ_l and τ_r , in conjunction with manual screening to curate a testset, *GeoTrust-test*, with 240 samples of varying levels of difficulty.

3.1. Data Distribution

TrustGeoGen was executed on a 60-core Intel Xeon (32) CPU @ 2.900GHz for two days, generating an initial dataset of 200K geometric reasoning instances in formal language. During the data generation process, we set the two filtering thresholds in the Sampler to $\tau_l = 5$ and $\tau_r = 0.5$, respectively. The distributions of the reasoning length and premises ratio for the resulting 200K dataset are illustrated in Fig. 3a and Fig. 3b, respectively. The majority of the data is concentrated in the region where the reasoning length is less than 60, and it decreases sharply beyond 80. However, a small portion of the data exhibits reasoning lengths exceeding 150, indicating a considerably high level of reasoning complexity. For a more detailed view of the distribution, please refer to the zoomed-in section of Fig. 3a.

3.2. Deep Reasoning Augmentation

As mentioned earlier, the randomly constructed scenarios by TrustGeoGen exhibit a rapid decline in reasoning length within the ultra-long range, posing challenges for generating deep-reasoning problems. To address this, we selected 226 samples with the longest reasoning lengths from an initial dataset of 200K and applied bootstrap augmentation to increase the proportion of deep-reasoning problems. Finally we obtained 376 geometric scenes after applying the bootstrap method. As shown in Fig. 3c, after the bootstrap

process, the data distribution in the region where reasoning length is smaller than 40 decreased, while it increased in the region where reasoning length is larger than 40. This method can be repeatedly applied to efficiently construct reasoning problems with significant depth and complexity.

3.3. Construction and Analysis of GeoTrust-Test

The synthetic data generated by TrustGeoGen can also be utilized to evaluate a model’s capabilities in the domain of deep geometric reasoning. From an initial dataset of 200K samples, we manually curated a set of 240 high-quality problems as the test set, graded by different levels of difficulty. As shown in Fig. 4, these problems are divided into four tiers, with each tier containing 60 problems. The reasoning lengths for *Tier*₁ range from 5 to 10 steps, *Tier*₂ spans from 10 to 20 steps, *Tier*₃ ranges from 20 to 50 steps, and *Tier*₄ exceeds 50 steps. It is worth noting that, to introduce distractors into the questions, the premises provided may not necessarily all be utilized in the reasoning process, resulting in a potentially lower premise ratio.

4. Experiment

To validate the quality and effectiveness of the geometric Problem Solving data generated by TrustGeoGen, we conducted experiments to explore:

- Whether existing MLLMs demonstrate competent performance on complex geometric problems?
- Whether geometric reasoning data with rigorous formal verification improve MLLMs’ capabilities and provide specific advantages?
- Whether *GeoTrust*, constructed without prior data sources, can generalize to OOD geometric testset?

4.1. Dataset, Metric, and Implementation Detail

Dataset. To evaluate the capability of MLLMs in solving complex geometry problems, we construct *GeoTrust-test* by partitioning the original *GeoTrust* dataset. As introduced in Sec. 3.3, the testset comprehensively covers four difficulty levels ranging from *Tier*₁ to *Tier*₄. To validate the effectiveness of our data construction, we additionally sample 3K geometry problems as *GeoTrust-train*, with each difficulty tier (*Tier*₁ to *Tier*₃[§]) containing 1K instances. GeoQA [6] is employed to evaluate the OOD generalization performance, comprising 4,998 geometric problems and solutions in natural language.

Metric. To eliminate potential evaluation bias introduced by the multiple-choice format, all input questions in the experiments are presented without answer options. Both the model’s final output answers and GT labels are extracted

[§]Considering the maximum output token limit of the trained open-source models, we excluded data from *Tier*₄.

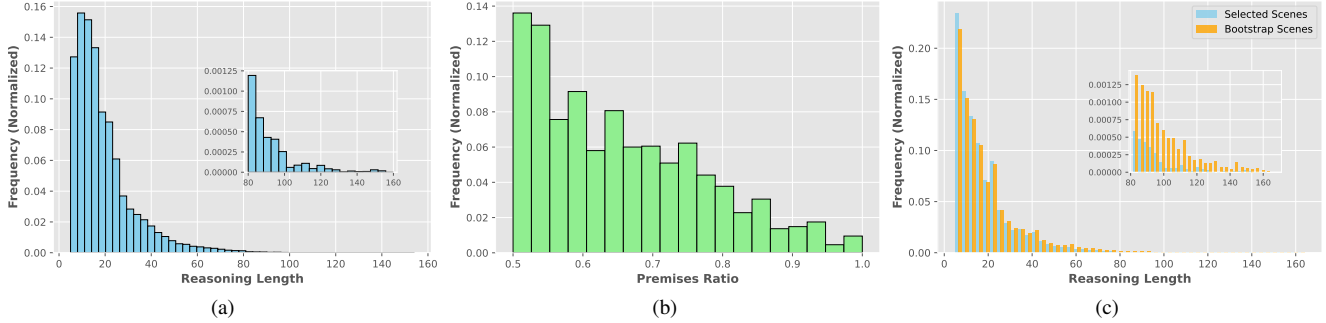


Figure 3. Data distribution and augmentation. (a) Distribution of reasoning lengths, with most samples below 60 steps and a sharp decline beyond 80; the zoomed-in view highlights the ultra-long reasoning range. (b) Distribution of premise ratios, reflecting variability in logical dependencies. (c) Comparison of reasoning lengths before and after bootstrap augmentation, showing increased deep-reasoning samples (reasoning length ≥ 40) and reduced shallow ones.

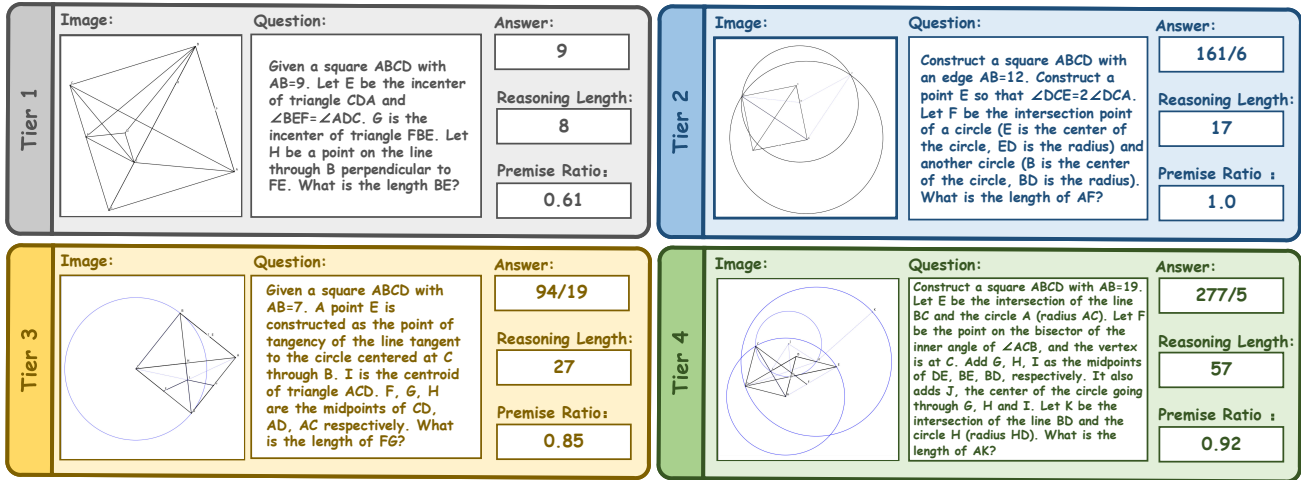


Figure 4. Visualization examples of different difficulty levels in *GeoTrust-test*, where "reasoning length" indicates step length of reasoning path and "premise ratio" refer to the ratio of premises unutilized during formal reasoning and premises provided in the question.

and converted into floating-point values for numerical comparison, with a relative error tolerance of 1% permitted.

Implementation Detail. In the experimental training protocol, all models are trained through supervised fine-tuning (SFT) with full-parameter updates for one epoch to prevent overfitting. All training and evaluation processes are conducted on 8 NVIDIA A100 (80G) GPUs.

4.2. Performance of Existing MLLMs

As shown in Tab. 1, the experimental results from the *GeoTrust-test* testset reveal critical insights into the capabilities of MLLMs in tackling complex geometric problems. Existing open-source models, such as Qwen2.5-VL-7B-Instruct [5], demonstrate significant limitations, achieving only a 12.92% overall accuracy (31/240), which also underscores the inherent challenges of the dataset and confirms its independence from prior biases in existing open-source testsets. Besides, closed-source commercial mod-

els like OpenAI-o1 [25] exhibit stronger reasoning capabilities, solving 109 problems (45.42% accuracy), though their performance sharply declines on higher-difficulty *Tier₄* questions (18.33% accuracy), highlighting persistent gaps in handling advanced geometric reasoning. Notably, the open-source reasoning model DeepSeek-R1[¶] [10] matches OpenAI-o1's overall accuracy, bridging the performance gap between open and closed-source systems and emphasizing the potential of scalable architectures. A consistent trend across all models is the progressive degradation of accuracy as problem difficulty escalates, validating the rigorous tiered difficulty framework of *GeoTrust-test*. These findings collectively emphasize the need for enhanced reasoning architectures and training paradigms to address the steep complexity gradient in geometric problem solving.

[¶]For DeepSeek-R1, we only provide natural language questions.

Table 1. Performance of state-of-the-art multi-modal language models on *GeoTrust-test*, which is divided into four difficulty levels.

Model	#Params	Total (out of 240)		<i>Tier</i> ₁ (out of 60)		<i>Tier</i> ₂ (out of 60)		<i>Tier</i> ₃ (out of 60)		<i>Tier</i> ₄ (out of 60)	
		num	acc	num	acc	num	acc	num	acc	num	acc
LLaVA-1.5 [19]	7B	7	2.91%	3	5.00%	2	3.33%	0	0.00%	2	3.33%
Qwen2-VL-Instruct [36]	7B	9	4.17%	5	8.33%	2	3.33%	0	0.00%	2	3.33%
Qwen2.5-VL-Instruct [5]	7B	24	10.00%	12	20.00%	6	10.00%	3	5.00%	3	5.00%
GPT-4o [24]	-	55	22.92%	25	41.67%	15	25.00%	9	15.00%	6	10.00%
Claude-3-7-Sonnet [3]	-	83	34.58%	35	58.33%	17	28.33%	24	40.00%	7	11.67%
DeepSeek-R1 [10]	671B	108	45.00%	40	66.67%	24	40.00%	25	41.67%	19	31.67%
OpenAI-o1 [25]	-	118	49.17%	42	70.00%	28	46.67%	26	43.33%	22	36.67%

Table 2. Comparison of performance on *GeoTrust-test* using trustworthy *GeoTrust-train* data and pseudo-labels annotated by OpenAI-o1 [25]. All trained on Qwen2-VL-7B-Instruct [5].

Training Data	Total	<i>Tier</i> ₁	<i>Tier</i> ₂	<i>Tier</i> ₃
-	7	5	2	0
pseudo-labels	21 (+14)	13 (+8)	3 (+1)	5 (+5)
100% <i>GeoTrust-train</i>	38 (+31)	27 (+22)	6 (+4)	5 (+5)
50% <i>GeoTrust-train</i>	27 (+20)	22 (+17)	4 (+2)	1 (+1)
30% <i>GeoTrust-train</i>	12 (+5)	10 (+5)	2 (-)	0 (-)

4.3. Advantages Provided by Trustworthy Data

To validate the effectiveness of the trustworthy data generated by TrustGeoGen, we compared our data with the ones generated by OpenAI-o1 [25]. We collect pseudo-labels generated by the OpenAI-o1 [25] via prompting the model with the problems in *GeoTrust-train*. We train Qwen2-VL-7B-Instruct [36] on both *GeoTrust-train* (with 100%, 50% and 30% data) and pseudo-labels, and report the number of problems solved from *Tier*₁ to *Tier*₃. As shown in Tab. 2, the model trained on 100% of *GeoTrust-train* outperforms the model trained on pseudo-labels, which demonstrates that trustworthy data hold substantial advantages over SOTA-generated pseudo-labels under equivalent data amount. Besides, as the amount of *GeoTrust-train* data increases, the model’s overall performance continues to improve, which further validates the effectiveness of our dataset. However, while the improvements on *Tier*₁ are notable, the gains on *Tier*₂ and *Tier*₃ remain significantly less pronounced, suggesting that supervised fine-tuning (SFT) does not produce substantial effects on more challenging geometric reasoning tasks.

4.4. OOD Generalization

The experiments are conducted on three pre-trained vision-language models: LLaVA-1.5-7B [19], LLaVA-1.5-13B [19] and Qwen2-VL-7B-Instruct [36]. For each model, we evaluate on GeoQA [6] with two training settings: (1) fine-tuning solely on the GeoQA dataset, and (2) fine-tuning with a combination of GeoQA and *GeoTrust-train* datasets to explore generalization. The results in Tab. 3

Table 3. OOD Generalization on GeoQA [6] when *GeoTrust-train* is leveraged for training, where Δ indicates the improvement compared to the pre-trained baseline.

Model	Training Data	acc	Δ
LLaVA-1.5-7B [19]	-	16.31%	-
	GeoQA	25.73%	+9.42%
	GeoQA+ <i>GeoTrust-train</i>	28.12%	+11.81%
LLaVA-1.5-13B [19]	-	18.83%	-
	GeoQA	29.84%	+11.01%
	GeoQA+ <i>GeoTrust-train</i>	33.16%	+14.33%
Qwen2-VL-7B-Instruct [36]	-	37.67%	-
	GeoQA	41.11%	+3.44%
	GeoQA+ <i>GeoTrust-train</i>	43.24%	+5.57%

demonstrate that incorporating *GeoTrust-train* data not only achieves substantial improvements over the original pre-trained models (e.g., +11.81% for LLaVA-1.5-7B and +5.57% for Qwen2-VL-7B), but also surpasses models fine-tuned solely on the in-distribution *GeoQA* training set. For example, LLaVA-1.5-7B improves from 25.73% accuracy (GeoQA-only fine-tuning) to 28.12% when augmented with *GeoTrust-train*, marking a +2.39% absolute gain over the in-distribution baseline, highlighting the generalization capability of our data.

5. Conclusion and Further Discussion

Conclusion. We present TrustGeoGen, a multimodal-integrated and scalable geometric data engine that automatically generates fully verified geometric reasoning data. The resulting *GeoTrust* dataset demonstrates validated effectiveness and generalization capabilities, with its trustworthy reasoning data showing significant advantages over conventional pseudo-labels. Notably, the *GeoTrust-test* exposes critical limitations of existing MLLMs in handling complex geometric reasoning tasks. GenGen represents a crucial first step towards trustworthy geometric problem solving, establishing a new paradigm for generating rigorous data.

Trustworthy Geometric Problem Solving. Models should produce verifiable reasoning steps, not merely correct answers. Achieving this demands both reliable data and robust evaluation mechanisms are required. Leveraging the generated data from TrustGeoGen, further study can

focus on autoformalization approaches that translate natural language reasoning into formalized steps, enabling automated verification of each deduction’s logical validity. Moreover, TrustGeoGen can dynamically generate evaluation data to prevent prior data leakage during evaluation, ensuring higher reliability in unseen geometric scenarios.

Formal Enhanced Reasoning. TrustGeoGen’s formalized reasoning environment enables the generation of trustworthy geometric data by constructing rigorous reasoning graphs that ensure logical correctness at each step. These graphs provide a structured foundation for exploring diverse mathematical reasoning strategies through tailored sampling methods: the current work implements multi-resolution and self-reflection traceback data, while future extensions could incorporate the idea of reverse thinking and categorical discussion, etc. These ideas could be further enhanced by integrating alternative training approaches (e.g. RL) to generalize to other reasoning scenarios.

References

- [1] Josh Achiam, Steven Adler, Sandhini Agarwal, Lama Ahmad, Ilge Akkaya, Florencia Leoni Aleman, Diogo Almeida, Janko Altenschmidt, Sam Altman, Shyamal Anadkat, et al. Gpt-4 technical report. *arXiv preprint arXiv:2303.08774*, 2023. 12
- [2] Josh Achiam, Steven Adler, Sandhini Agarwal, Lama Ahmad, Ilge Akkaya, Florencia Leoni Aleman, Diogo Almeida, Janko Altenschmidt, Sam Altman, Shyamal Anadkat, et al. Gpt-4 technical report. *arXiv preprint arXiv:2303.08774*, 2023. 1
- [3] Anthropic. The claude 3 model family: Opus, sonnet, haiku. <https://www.anthropic.com/>, 2024. 8, 12
- [4] Jinze Bai, Shuai Bai, Shusheng Yang, Shijie Wang, Sinan Tan, Peng Wang, Junyang Lin, Chang Zhou, and Jingren Zhou. Qwen-vl: A frontier large vision-language model with versatile abilities. *arXiv preprint arXiv:2308.12966*, 2023. 1, 12
- [5] Shuai Bai, Keqin Chen, Xuejing Liu, Jialin Wang, Wenbin Ge, Sibao Song, Kai Dang, Peng Wang, Shijie Wang, Jun Tang, Humen Zhong, Yuanzhi Zhu, Mingkun Yang, Zhaohai Li, Jianqiang Wan, Pengfei Wang, Wei Ding, Zheren Fu, Yiheng Xu, Jiabo Ye, Xi Zhang, Tianbao Xie, Zesen Cheng, Hang Zhang, Zhibo Yang, Haiyang Xu, and Junyang Lin. Qwen2.5-vl technical report. *ArXiv*, abs/2502.13923, 2024. 7, 8
- [6] Jiaqi Chen, Jianheng Tang, Jinghui Qin, Xiaodan Liang, Lingbo Liu, Eric Xing, and Liang Lin. Geoqa: A geometric question answering benchmark towards multimodal numerical reasoning. In *Findings of the Association for Computational Linguistics: ACL-IJCNLP 2021*, pages 513–523, 2021. 1, 3, 6, 8, 12
- [7] Jiaqi Chen, Tong Li, Jinghui Qin, Pan Lu, Liang Lin, Chongyu Chen, and Xiaodan Liang. Unigeo: Unifying geometry logical reasoning via reformulating mathematical expression. In *Proceedings of the 2022 Conference on Empirical Methods in Natural Language Processing*, pages 3313–3323, 2022. 1, 12
- [8] Zhe Chen, Jiannan Wu, Wenhai Wang, Weijie Su, Guo Chen, Sen Xing, Muyan Zhong, Qinglong Zhang, Xizhou Zhu, Lewei Lu, et al. Internvl: Scaling up vision foundation models and aligning for generic visual-linguistic tasks. In *Proceedings of the IEEE/CVF conference on computer vision and pattern recognition*, pages 24185–24198, 2024. 1
- [9] Yuri Chervonyi, Trieu H. Trinh, Miroslav Olišák, Xiaomeng Yang, Hoang Nguyen, Marcelo Menegali, Junehyuk Jung, Vikas Verma, Quoc V. Le, and Thang Luong. Gold-medalist performance in solving olympiad geometry with alpheageometry2. *ArXiv*, 2502.03544, 2025. 1, 12
- [10] DeepSeek-AI, Daya Guo, Dejian Yang, Haowei Zhang, Junmei Song, Ruoyu Zhang, Runxin Xu, Qihao Zhu, Shirong Ma, Peiyi Wang, Xiaoling Bi, Xiaokang Zhang, Xingkai Yu, Yu Wu, Z. F. Wu, Zhibin Gou, Zhihong Shao, Zhuoshu Li, Ziyi Gao, Aixin Liu, Bing Xue, Bing-Li Wang, Bochao Wu, Bei Feng, Chengda Lu, Chenggang Zhao, Chengqi Deng, Chenyu Zhang, Chong Ruan, Damai Dai, Deli Chen, Dong-Li Ji, Erhang Li, Fangyun Lin, Fucong Dai, Fuli Luo, Guangbo Hao, Guanting Chen, Guowei Li, H. Zhang, Han Bao, Hanwei Xu, Haocheng Wang, Honghui Ding, Huajian Xin, Huazuo Gao, Hui Qu, Hui Li, Jianzhong Guo, Jiashi Li, Jiawei Wang, Jingchang Chen, Jingyang Yuan, Junjie Qiu, Junlong Li, Jiong Cai, Jiaqi Ni, Jian Liang, Jin Chen, Kai Dong, Kai Hu, Kaige Gao, Kang Guan, Kexin Huang, Kuai Yu, Lean Wang, Lecong Zhang, Liang Zhao, Litong Wang, Liyue Zhang, Lei Xu, Leyi Xia, Mingchuan Zhang, Minghua Zhang, M. Tang, Meng Li, Miaojun Wang, Mingming Li, Ning Tian, Panpan Huang, Peng Zhang, Qiancheng Wang, Qinyu Chen, Qiushi Du, Ruiqi Ge, Ruisong Zhang, Ruizhe Pan, Runji Wang, R. J. Chen, R. L. Jin, Ruyi Chen, Shanghao Lu, Shangyan Zhou, Shanhuang Chen, Shengfeng Ye, Shiyu Wang, Shuiping Yu, Shunfeng Zhou, Shuting Pan, S. S. Li, Shuang Zhou, Shao-Kang Wu, Tao Yun, Tian Pei, Tianyu Sun, T. Wang, Wangding Zeng, Wanbiao Zhao, Wen Liu, Wenfeng Liang, Wenjun Gao, Wen-Xia Yu, Wentao Zhang, W. L. Xiao, Wei An, Xiaodong Liu, Xiaohan Wang, Xiaokang Chen, Xiaotao Nie, Xin Cheng, Xin Liu, Xin Xie, Xingchao Liu, Xinyu Yang, Xinyuan Li, Xuecheng Su, Xuheng Lin, X. Q. Li, Xiangyu Jin, Xi-Cheng Shen, Xiaosha Chen, Xiaowen Sun, Xiaoxiang Wang, Xinnan Song, Xinyi Zhou, Xianzu Wang, Xinxia Shan, Y. K. Li, Y. Q. Wang, Y. X. Wei, Yang Zhang, Yanhong Xu, Yao Li, Yao Zhao, Yaofeng Sun, Yaohui Wang, Yi Yu, Yichao Zhang, Yifan Shi, Yi Xiong, Ying He, Yishi Piao, Yisong Wang, Yixuan Tan, Yiyang Ma, Yiyuan Liu, Yongqiang Guo, Yuan Ou, Yuduan Wang, Yue Gong, Yu-Jing Zou, Yujia He, Yunfan Xiong, Yu-Wei Luo, Yu mei You, Yuxuan Liu, Yuyang Zhou, Y. X. Zhu, Yanping Huang, Yao Li, Yi Zheng, Yuchen Zhu, Yunxiang Ma, Ying Tang, Yukun Zha, Yuting Yan, Zehui Ren, Zehui Ren, Zhangli Sha, Zhe Fu, Zhean Xu, Zhenda Xie, Zhen guo Zhang, Zhewen Hao, Zhicheng Ma, Zhigang Yan, Zhiyu Wu, Zihui Gu, Zijia Zhu, Zijun Liu, Zi-An Li, Ziwei Xie, Ziyang Song, Zizheng Pan, Zhen Huang, Zhipeng Xu, Zhongyu Zhang, and Zhen Zhang. Deepseek-r1: Incentivizing reasoning capability in llms via reinforcement learning. *ArXiv*, abs/2501.12948, 2025. 2, 7, 8, 12

- [11] Xiaoyi Dong, Pan Zhang, Yuhang Zang, Yuhang Cao, Bin Wang, Linke Ouyang, Xilin Wei, Songyang Zhang, Haodong Duan, Maosong Cao, Wenwei Zhang, Yining Li, Hang Yan, Yang Gao, Xinyue Zhang, Wei Li, Jingwen Li, Kai Chen, Conghui He, Xingcheng Zhang, Yu Qiao, Dahua Lin, and Jiaqi Wang. Internlm-xcomposer2: Mastering free-form text-image composition and comprehension in vision-language large model. *ArXiv*, abs/2401.16420, 2024. 1
- [12] Xiaoyi Dong, Pan Zhang, Yuhang Zang, Yuhang Cao, Bin Wang, Linke Ouyang, Songyang Zhang, Haodong Duan, Wenwei Zhang, Yining Li, Hang Yan, Yang Gao, Zhe Chen, Xinyue Zhang, Wei Li, Jingwen Li, Wenhai Wang, Kai Chen, Conghui He, Xingcheng Zhang, Jifeng Dai, Yu Qiao, Dahua Lin, and Jiaqi Wang. Internlm-xcomposer2-4khd: A pioneering large vision-language model handling resolutions from 336 pixels to 4k hd. *ArXiv*, abs/2404.06512, 2024. 1
- [13] Chaoyou Fu, Peixian Chen, Yunhang Shen, Yulei Qin, Mengdan Zhang, Xu Lin, Jinrui Yang, Xiawu Zheng, Ke Li, Xing Sun, et al. Mme: A comprehensive evaluation benchmark for multimodal large language models. *arXiv preprint arXiv:2306.13394*, 2023. 12
- [14] Jiahui Gao, Renjie Pi, Jipeng Zhang, Jiacheng Ye, Wanjun Zhong, Yufei Wang, Lanqing Hong, Jianhua Han, Hang Xu, Zhenguo Li, et al. G-llava: Solving geometric problem with multi-modal large language model. In *The Thirteenth International Conference on Learning Representations*, 2025. 1, 12
- [15] Yihan Hao, Mingliang Zhang, Fei Yin, and Lin-Lin Huang. Pgd5k: A diagram parsing dataset for plane geometry problems. In *2022 26th International Conference on Pattern Recognition (ICPR)*, pages 1763–1769. IEEE, 2022. 1
- [16] Dongzhi Jiang, Renrui Zhang, Ziyu Guo, Yanwei Li, Yu Qi, Xinyan Chen, Liuhui Wang, Jianhan Jin, Claire Guo, Shen Yan, et al. Mme-cot: Benchmarking chain-of-thought in large multimodal models for reasoning quality, robustness, and efficiency. *arXiv preprint arXiv:2502.09621*, 2025. 12
- [17] Junnan Li, Dongxu Li, Silvio Savarese, and Steven Hoi. Blip-2: Bootstrapping language-image pre-training with frozen image encoders and large language models. In *International conference on machine learning*, pages 19730–19742. PMLR, 2023. 12
- [18] Zhenwen Liang, Tianyu Yang, Jipeng Zhang, and Xiangliang Zhang. Unimath: A foundational and multimodal mathematical reasoner. In *Proceedings of the 2023 Conference on Empirical Methods in Natural Language Processing*, pages 7126–7133, 2023. 1
- [19] Haotian Liu, Chunyuan Li, Qingyang Wu, and Yong Jae Lee. Visual instruction tuning. *Advances in neural information processing systems*, 36, 2024. 8, 12
- [20] Haoyu Lu, Wen Liu, Bo Zhang, Bingxuan Wang, Kai Dong, Bo Liu, Jingxiang Sun, Tongzheng Ren, Zhuoshu Li, Hao Yang, et al. Deepseek-vl: towards real-world vision-language understanding. *arXiv preprint arXiv:2403.05525*, 2024. 1
- [21] Pan Lu, Ran Gong, Shibiao Jiang, Liang Qiu, Siyuan Huang, Xiaodan Liang, and Song-Chun Zhu. Inter-gps: Interpretable geometry problem solving with formal language and symbolic reasoning. *arXiv preprint arXiv:2105.04165*, 2021. 1
- [22] Pan Lu, Hritik Bansal, Tony Xia, Jiacheng Liu, Chunyuan Li, Hannaneh Hajishirzi, Hao Cheng, Kai-Wei Chang, Michel Galley, and Jianfeng Gao. Mathvista: Evaluating mathematical reasoning of foundation models in visual contexts. In *The Twelfth International Conference on Learning Representations*, 2024. 1, 12
- [23] OpenAI. Gpt-4v. <https://openai.com/index/gpt-4v-system-card/>, 2023. 1
- [24] OpenAI. Hello gpt-4o. <https://openai.com/index/hello-gpt-4o/>, 2024. 1, 8, 12
- [25] OpenAI. Gpt-o1. <https://openai.com/index/openai-o1-system-card/>, 2024. 2, 3, 7, 8, 12
- [26] Long Ouyang, Jeffrey Wu, Xu Jiang, Diogo Almeida, Carroll Wainwright, Pamela Mishkin, Chong Zhang, Sandhini Agarwal, Katarina Slama, Alex Ray, et al. Training language models to follow instructions with human feedback. *Advances in neural information processing systems*, 35:27730–27744, 2022. 12
- [27] Tianshuo Peng, Mingsheng Li, Hongbin Zhou, Renqiu Xia, Renrui Zhang, Lei Bai, Song Mao, Bin Wang, Conghui He, Aojun Zhou, Botian Shi, Tao Chen, Bo Zhang, and Xiangyu Yue. Chimera: Improving generalist model with domain-specific experts. *ArXiv*, abs/2412.05983, 2024. 1
- [28] Tianshuo Peng, Mingsheng Li, Hongbin Zhou, Renqiu Xia, Renrui Zhang, Lei Bai, Song Mao, Bin Wang, Conghui He, Aojun Zhou, et al. Chimera: Improving generalist model with domain-specific experts. *arXiv preprint arXiv:2412.05983*, 2024. 1
- [29] Machel Reid, Nikolay Savinov, Denis Teplyashin, Dmitry Lepikhin, Timothy Lillicrap, Jean-baptiste Alayrac, Radu Soricut, Angeliki Lazaridou, Orhan Firat, Julian Schrittwieser, et al. Gemini 1.5: Unlocking multimodal understanding across millions of tokens of context. *arXiv preprint arXiv:2403.05530*, 2024. 12
- [30] Wenhao Shi, Zhiqiang Hu, Yi Bin, Junhua Liu, Yang Yang, See-Kiong Ng, Lidong Bing, and Roy Ka-Wei Lee. Mathllava: Bootstrapping mathematical reasoning for multimodal large language models. *arXiv preprint arXiv:2406.17294*, 2024. 1
- [31] Vladimir Sicca, Tianxiang Xia, Mathis Fédérico, Philip John Gorinski, Simon Frieder, and Shangling Jui. Newclid: A user-friendly replacement for alphageometry. *arXiv preprint arXiv:2411.11938*, 2024. 3, 12
- [32] InternLM Team. Internlm: A multilingual language model with progressively enhanced capabilities, 2023. 12
- [33] Hugo Touvron, Thibaut Lavril, Gautier Izacard, Xavier Martinet, Marie-Anne Lachaux, Timothée Lacroix, Baptiste Rozière, Naman Goyal, Eric Hambro, Faisal Azhar, et al. Llama: Open and efficient foundation language models. *arXiv preprint arXiv:2302.13971*, 2023.
- [34] Hugo Touvron, Louis Martin, Kevin Stone, Peter Albert, Amjad Almahairi, Yasmine Babaei, Nikolay Bashlykov, Soumya Batra, Prajjwal Bhargava, Shruti Bhosale, et al. Llama 2: Open foundation and fine-tuned chat models. *arXiv preprint arXiv:2307.09288*, 2023. 12
- [35] Trieu Trinh, Yuhuai Wu, Quoc Le, He He, and Thang Luong. Solving olympiad geometry without human demonstrations. *Nature*, 2024. 1, 12

- [36] Peng Wang, Shuai Bai, Sinan Tan, Shijie Wang, Zihao Fan, Jinze Bai, Keqin Chen, Xuejing Liu, Jialin Wang, Wenbin Ge, Yang Fan, Kai Dang, Mengfei Du, Xuancheng Ren, Rui Men, Dayiheng Liu, Chang Zhou, Jingren Zhou, and Junyang Lin. Qwen2-vl: Enhancing vision-language model’s perception of the world at any resolution. *ArXiv*, abs/2409.12191, 2024. 8
- [37] Zhiyu Wu, Xiaokang Chen, Zizheng Pan, Xingchao Liu, Wen Liu, Damai Dai, Huazuo Gao, Yiyang Ma, Chengyue Wu, Bingxuan Wang, Zhenda Xie, Yu Wu, Kai Hu, Jiawei Wang, Yaofeng Sun, Yukun Li, Yishi Piao, Kang Guan, Aixin Liu, Xin Xie, Yuxiang You, Kai Dong, Xingkai Yu, Haowei Zhang, Liang Zhao, Yisong Wang, and Chong Ruan. Deepseek-vl2: Mixture-of-experts vision-language models for advanced multimodal understanding, 2024. 1
- [38] Renqiu Xia, Bo Zhang, Haoyang Peng, Ning Liao, Peng Ye, Botian Shi, Junchi Yan, and Yu Qiao. Structchart: Perception, structuring, reasoning for visual chart understanding. *arXiv preprint arXiv:2309.11268*, 2023. 12
- [39] Renqiu Xia, Song Mao, Xiangchao Yan, Hongbin Zhou, Bo Zhang, Haoyang Peng, Jiahao Pi, Daocheng Fu, Wenjie Wu, Hancheng Ye, et al. Docgenome: An open large-scale scientific document benchmark for training and testing multi-modal large language models. *arXiv preprint arXiv:2406.11633*, 2024. 12
- [40] Renqiu Xia, Mingsheng Li, Hancheng Ye, Wenjie Wu, Hongbin Zhou, Jiakang Yuan, Tianshuo Peng, Xinyu Cai, Xiangchao Yan, Bin Wang, Conghui He, Botian Shi, Tao Chen, Junchi Yan, and Bo Zhang. Geox: Geometric problem solving through unified formalized vision-language pre-training. In *The Thirteenth International Conference on Learning Representations*, 2025. 1, 12
- [41] Ling Yang, Zhaochen Yu, Bin Cui, and Mengdi Wang. Reasonflux: Hierarchical llm reasoning via scaling thought templates. *arXiv preprint arXiv:2502.06772*, 2025. 5
- [42] Yixin Ye, Zhen Huang, Yang Xiao, Ethan Chern, Shijie Xia, and Pengfei Liu. Limo: Less is more for reasoning. *arXiv preprint arXiv:2502.03387*, 2025. 5
- [43] Chi Zhang, Jiajun Song, Siyu Li, Yitao Liang, Yuxi Ma, Wei Wang, Yixin Zhu, and Song-Chun Zhu. Proposing and solving olympiad geometry with guided tree search. *ArXiv*, abs/2412.10673, 2024. 1
- [44] Ming-Liang Zhang, Fei Yin, and Cheng-Lin Liu. A multimodal neural geometric solver with textual clauses parsed from diagram. *arXiv preprint arXiv:2302.11097*, 2023. 1, 12
- [45] Pan Zhang, Xiaoyi Dong, Yuhang Zang, Yuhang Cao, Rui Qian, Lin Chen, Qipeng Guo, Haodong Duan, Bin Wang, Linke Ouyang, Songyang Zhang, Wenwei Zhang, Yining Li, Yang Gao, Peng Sun, Xinyue Zhang, Wei Li, Jingwen Li, Wenhai Wang, Hang Yan, Conghui He, Xingcheng Zhang, Kai Chen, Jifeng Dai, Yu Qiao, Dahua Lin, and Jiaqi Wang. Internlm-xcomposer-2.5: A versatile large vision language model supporting long-contextual input and output. *ArXiv*, abs/2407.03320, 2024. 1
- [46] Renrui Zhang, Xinyu Wei, Dongzhi Jiang, Yichi Zhang, Ziyu Guo, Chengzhuo Tong, Jiaming Liu, Aojun Zhou, Bin Wei, Shanghang Zhang, et al. Mavis: Mathematical visual instruction tuning. *arXiv preprint arXiv:2407.08739*, 2024. 1, 12

Appendix

A. Related Work

Advances in Multimodal Large Language Model. Recent advances in Large Language Models (LLMs) have demonstrated remarkable progress in linguistic intelligence, achieving human-level capabilities in various applications [26, 32–34]. Building upon this foundation, the research community has focused on extending these text-based architectures to process visual information, leading to the emergence of sophisticated Multimodal Large Language Models (MLLMs) [1, 4, 29]. These integrated systems typically employ modality alignment mechanisms, such as Q-former [17] and linear layers [19], to establish connections between visual representations and text embeddings. Although current MLLMs show strong performance in standard vision-language benchmarks [13, 16, 22, 38, 39], their effectiveness decreases significantly when processing mathematical visualizations that require reasoning. Recent specialized approaches address this limitation through targeted training strategies. For example, geometric reasoning capabilities have been enhanced through domain-specific datasets containing annotated diagrams [14, 46].

Geometric Problem Solving. As a challenging task, geometric problem solving requires understanding diagrams, interpreting symbols, and performing complex reasoning. While MLLMs have shown remarkable proficiency in human-level reasoning and generation capabilities, they struggle with automatic geometric problem solving due to their pre-training on natural images and texts, as well as the lack of automated verification in the problem-solving process. To address this limitation, researchers have proposed various approaches to improve the understanding of geometric images and corpora, including unimodal pre-training, vision-language alignment, and visual instruction tuning [6, 7, 14–16, 40, 44, 46]. Another major approach involves the use of formalized solvers to tackle geometric problems. While these solvers [9, 31, 35] are capable of addressing challenges at the level of the International Mathematical Olympiad (IMO), they require precise modeling of geometric problems to fit the solver’s language. This necessity introduces significant obstacles in terms of practical

Model Name	Model / API Version
GPT-4o [24]	gpt-4o-2024-11-20
Claude-3-7-Sonnet [3]	claude-3-7-sonnet-20250219
DeepSeek-R1 [10]	deepseek-r1
OpenAI-o1 [25]	o1-2024-12-17

Table 4. Model / API versions used for evaluation across different MLLMs.

application and generalization, limiting the usability in real-world scenarios.

B. Versions of Closed-source Model

During the evaluation on *GeoTrust-test*, we utilize some closed-source commercial models, with the specific version detailed in Table 4.

C. More Visualization Example

In Fig. 5, we provide one more visualization example in *GeoTrust* with 94 reasoning steps and 0.95 premises ratio.

Image:

Question:

ABCD is a square with side length $AB=17$. Points E, F, and G are the midpoints of sides DC, DB and BC, respectively. Let H be the center of the circle passing through points E, F, and G. Let I be the center of the circle passing through points B, C, and H. Find the length of EI.

Solution:

Step 0: Since F is the midpoint of BD and E is the midpoint of DC, it follows that $DF:DB = DE:DC$. Therefore, EF is parallel to BC ($EF \parallel BC$).

Step 1: Since $EF \parallel BC$, we have $\angle DFE = \angle DBC$.

Step 2: Given that $DC = CB$ and that points D, E, and C are collinear, as well as points D, F, and B, we can conclude $\angle DBC = \angle CDB = \angle EDF$.

Step 3: Since $\angle DBC = \angle EDF$ and $\angle DFE = \angle DBC$, it follows that $\angle EDF = \angle DFE$, which implies $DE = EF$.

...

Step 91: Since $AH \perp GH$, $AG = 19$, and $GH = 6.02$, we can compute $AH = 18.05$, and subsequently $FI = 12.75$.

Step 92: Given that F, G, and I are collinear, $AB \parallel CD$, $BC \parallel EF$, $CD \parallel FG$, and $AB \perp BC$, it follows that $EF \perp FI$.

Step 93: Since $EF \perp FI$, $EF = 8.5$, and $FI = 12.75$, we find that $EI = 15.33$.

Figure 5. One visualization example in *GeoTrust*.